Marine Pollution Bulletin 189 (2023) 114807

Contents lists available at ScienceDirect

Marine Pollution Bulletin

journal homepage: www.elsevier.com/locate/marpolbul

On-field high-resolution quantification of the cobalt fraction available for bio-uptake in natural waters using antifouling gel-integrated microelectrode arrays

Nicolas Layglon *, Sébastien Creffield, Eric Bakker, Mary-Lou Tercier-Waeber *

Department of Inorganic and Analytical Chemistry, University of Geneva, Quai E.-Ansermet 30, 1211 Geneva, Switzerland

ARTICLE INFO

Keywords:
Cobalt
Dynamic Co-nioxime fraction
Adsorptive Square Wave Cathodic Stripping Voltammetry (Ad-SWCSV)
Aquatic systems

ABSTRACT

We report the optimization, characterization, and validation of Adsorptive Square Wave Cathodic Stripping Voltammetry on antifouling gel-integrated microelectrode arrays for autonomous, direct monitoring of cobalt(II) metal species. Detection is accomplished by complexation with an added nioxime ligand. The limit of detection established for a 90 s accumulation time was 0.29 ± 0.01 nM in freshwater and 0.27 ± 0.06 nM in seawater. The microelectrode array was integrated in a submersible probe to automatically dose the complexing agent nioxime and realize an integrated sensing system. For the first time ever, the potentially bioavailable Co(II) fraction was determined in La Leyre River-Arcachon Bay continuum, enabling to evaluate the potential ecotoxicological impact of freshwater-carried Co(II) in the Arcachon Bay. The measured potentially bioavailable Co(II) concentrations were hazardous for aquatic biota along the continuum. The electrochemical Co(II) data were compared to ICP-MS data in various fractions to determine spatial Co(II) speciation.

1. Introduction

The anthropogenic release of ubiquitous and persistent trace metals increased exponentially since the industrial revolution. Among these, cobalt (Co) is an important bioactive trace metal (Bundy et al., 2020). In a given range of concentration, Co plays a critical role in phytoplankton growth and calcification (Anderson et al., 2014; Bundy et al., 2020) and may catalyze cellular processes for carbon fixation and organic phosphorus acquisition (Tagliabue et al., 2018). Above or below this optimal concentration range, Co can cause deleterious effects to aquatic organisms (Saili et al., 2021). Unfortunately, today no provisional guidelines for the regulation of cobalt exist by the European Water Directive (WFD-2013/39/EU, 2013). However, the Australian and New-Zealand governments have established threshold concentrations for hazardous compounds to protect marine species and reported that available Co concentrations should not exceed 0.085 nM (to protect 99 % of the aquatic species) and 17 nM (to protect 95 % of the aquatic species) in seawater, respectively (ANZEEC, 2000). Cobalt concentrations in fresh water can be as low as 0.1 nM and reach up to 1.28 mM in impacted areas (Kosiorek, 2019). Because seawater Co concentrations range from 0.017 nM in the open sea to 12.8 nM in coastal areas, appropriate guidelines for cobalt are needed.

In the aquatic environment Co(II) is the dominant oxidation state owing to low Co(III) solubility (Collins and Kinsela, 2010) and can be found in different chemical forms or species. Based on size, three homologous fractions can be defined as particulate (size ≥0.2 μm), colloidal (0.2 μm ≥ size ≤ 1 nm) and the truly dissolved fraction (size <1 nm). This later includes the free metal ions and the labile complexes that are potentially bioavailable. The proportion of these different forms are influenced by the physicochemical conditions, the water composition and various biotic and abiotic processes and may vary continuosly in space and time (Abdou et al., 2022; Abdou and Tercier-Waeber, 2022; Layglon et al., 2022; Tercier-Waeber et al., 2009, 2021b).

Sensing systems that enable the *in situ*, autonomous measurements of bioavailable metals at appropriate frequency are needed for improving metal ecological risk assessments. The implementation of a more efficient environmental regulation was indeed recently prescribed by EU and international administrations (WCA Environment, 2015, 2016). Today, the techniques recommended by government institutions to define metal concentration guidelines to protect aquatic ecosystems include DGT (Diffusive Gradient in Thin Films) (Cindric et al., 2017) and computer code speciation models, especially the Biotic Ligand Model (BLM). DGT provides only averaged concentrations over the total deployment time (usually 2 to 5 days) (Väänänen et al., 2018 and ref.

* Corresponding authors.
E-mail addresses: nicolas.layglon@unige.ch (N. Layglon), marie-louise.tercier@unige.ch (M.-L. Tercier-Waeber).

https://doi.org/10.1016/j.marpolbul.2023.114807
Received 3 December 2022; Received in revised form 1 March 2023; Accepted 3 March 2023
Available online 14 March 2023

therein). BLM assumes that the free hydrated ion in solution is the only chemical species available for biouptake (Niyogi and Wood, 2004) which is not always true (*e.g.* (Tercier-Waeber et al., 2012; Zhao et al., 2016; and refs therein). Reliable site-specific BLM data requires a high number of input parameters (T, pH, DOC, major inorganic cations and anions, alkalinity and sulfides, DOC, fulvic and humic acid proportion of DOC; Smith et al., 2015). BLM also suffers from the uncertainty of complexation/adsorption constants of metals with complex natural inorganic or organic ligands/sorbents. These drawbacks can only be solved by the development of cost-effective methods that allow for the direct *in situ* quantification of potentially bioavailable metal species. The characteristics of voltammetric techniques are well suited for this purpose (Buffle and Tercier-Waeber, 2000, 2005).

Anodic Stripping Voltammetry (ASV) uses an electrochemical preconcentration step while in Adsorptive Cathodic Stripping Voltammetry (Ad-CSV) the preconcentration of metal complexes is achieved chemically by adding an appropriate ligand to the sample. These two approaches were first developed on macroelectrodes (mainly hanging mercury drops) and made it possible to reach sensitivities of the order of pM (Buffle and Tercier-Waeber, 2000; Pađan et al., 2019, 2020). Later on, both approaches have been used with microelectrodes, to quantify trace metals in natural waters (Holmes et al., 2019; Kokkinos and Economou, 2016; Tercier-Waeber and Buffle, 2013; Wang et al., 2000; Xie et al., 2005). One of the main features of microelectrodes is that they exhibit hemispherical diffusion that results in an attractive non-zero steady-state currents in quiescent solution during the ASV and Ad-CSV metal preconcentration steps (Bard and Faulkner, 2001; Buffle and Tercier-Waeber, 2000). However, most of these developments focused on the quantification of the total dissolved metal concentration. Moreover, the drawbacks for their *in situ* application at natural pH are their susceptibility to adsorb organic matter and suspended colloids/particles resulting in fouling, and to poorly controlled convective conditions in the sample (Belmont-Hebert et al., 1998; Gibbon-Walsh et al., 2010; Tercier and Buffle, 1996; Tercier-Waeber and Buffle, 2013; Tercier-Waeber et al., 2008; Touilloux et al., 2015). These drawbacks can be overcome with gel-integrated microelectrodes (GIME), forming an array of interconnected Ir-microdisc of radius $\leq$ 10 μm, electroplated with appropriate sensing elements and covered by a hydrogel membrane (Belmont-Hebert et al., 1998; Tercier and Buffle, 1996; Tercier-Waeber et al., 2021a, 2021c; Touilloux et al., 2015). The agarose gel can be understood to mimic the membrane of living cells (Buffle and Tercier-Waeber, 2005). It efficiently excludes compounds >15 nm that represent typical fouling materials. The gel also forms a stagnant layer and helps to eliminate the influence of sample convection (Belmont-Hebert et al., 1998; Tercier-Waeber et al., 2021a). These characteristics allow GIME sensors to perform reliable, high-resolution and long-term measurements in complex aquatic media without the need to renew the sensing element (Tercier-Waeber et al., 2009, 2021c). Because of the dynamic nature of the measurement, which depends on kinetically labile species that diffuse across the gel layer, GIME may be understood as directly detecting the so-called dynamic metal species, *i.e.*, the sum of the free metal ions and the sufficiently labile and mobile (size $\leq$4 nm) metal species in solution (Buffle and Tercier-Waeber, 2005). This fraction represents the total dissolved metal species available for biouptake by microorganisms (Buffle and Tercier-Waeber, 2005; Tercier-Waeber et al., 2012 and refs. therein). Incorporated in submersible sensing probes applied *in situ* or on-board (Tercier-Waeber et al., 2021b; Tercier-Waeber and Taillefert, 2008), the GIME can be used to study the processes that may influence the concentration of the dynamic metal species and to better assess metal potential ecotoxicological impact (Abdou et al., 2022; Abdou and Tercier-Waeber, 2022; Illuminati et al., 2019; Layglon et al., 2022; Masson and Tercier-Waeber, 2014; Tercier-Waeber et al., 2021a, b, c). However, until today, only metals electrochemically preconcentrated at a GIME using ASV techniques have been studied with this technology. The adaptation of Adsorptive Cathodic Stripping Voltammetry at a GIME would be very valuable for detecting metal species that can only be observed electrochemically following a chemical preconcentration step upon complexation with an appropriate ligand (Tercier-Waeber and Buffle, 2013 and refs. therein).

In this study, we investigated and optimized the performance of Adsorptive Square Wave Cathodic Stripping Voltammetry on a gel-integrated Hg-plated Ir-based microelectrode array (Hg-GIME) to quantify dissolved Co(II) metal species available for biouptake. This was achieved by chemical preconcentration after sample addition of the ligand nioxime, which has been shown to give improved results compared to dimethylglyoxime (Vega and van den Berg, 1997). Various parameters that may influence the *in situ* voltammetric quantification of the mobile and kinetically labile (dynamic) Co-nioxime complex were investigated, including the nioxime concentration, pH, temperature and contrasting media composition (synthetic media, fresh and marine natural waters). The Hg-GIME and sample manipulation steps were then integrated into a submersible Voltammetric *In situ* Profiling system (Tercier et al., 1998), which was then applied for direct measurements of dynamic Co-nioxime species in the La Leyre-Arcachon Bay fluvial-estuarine system (France) during ebb tide. Ancillary analysis of total dissolved Co(II) concentrations in raw and filtered (0.2 and 0.02 μm) samples as well as water composition were also performed. The collected data were used to determine spatial Co speciation, to evaluate the capability of the Hg-GIME VIP system to identify potential sources of Co(II) species available for bio-uptake, and to assess the ecotoxicity impact of Co(II) carried by surface waters in the Arcachon Bay, which is an important regional ecosystem for oyster production.

2. Experimental

2.1. Chemicals and instrumentation

All solutions were prepared with ultra-pure deionized water (Milli-Q, 18.2 mΩ·cm from a Fisher system). Boric acid (H_3BO_3), nitric acid (HNO_3) and sodium hydroxide (NaOH) were suprapur grade (Merck) while $Hg(CH_3COO)_2$ and KSCN were analytical-grade (Merk). Standard stock solution of 1 g L^{-1} Co(II) (*Trace*CERT®, 2 % w/w HNO_3, Sigma Aldrich), 1,2-Cyclohexanedione dioxime (Nioxime 97 %, Alfa Aeser) as well as agarose (LGL agarose, Biofinex®-Switzerland) were used. A stock solution of 10 mM nioxime was prepared by dissolving nioxime in Milli-Q water and was stored protected to sunlight by aluminum foil at 4 °C. Standard solutions of Co were prepared by dilution from the stock standard solution.

The measurements to evaluate the influence of the temperature on the electrical signal were performed using a thermostated glass cell (Metrohm) coupled to a Julabo F34 thermostated water bath. The precision on the temperature measured was on the order of 1 °C.

The total Co concentrations in the various fractions were measured by ICP-MS (iCAP TQ ICP-MS Thermo®). A certified reference material (CASS-6, Nearshore seawater reference material for trace metals, National Research Council Canada) was used as a quality control of ICP-MS measurements. The recovery was 104 ± 2 %.

2.2. On-chip sensors preparation and renewal

Hg-GIME were prepared from on-chip array of 5 × 20 interconnected Ir-based microdiscs of 2.5 μm in radius and a center-to-center inter-distance of 150 μm surrounded by a 300 μm-thick EPON SU8 ring in which a high purity agarose gel (LGL agarose), acting as efficient anti-fouling membrane, is deposited (Belmont-Hebert et al., 1998; Tercier and Buffle, 1996). The antifouling agarose gel deposition was performed by dipping the chip in a 1.5 % LGL agarose solution heated at 80 °C. A homogeneous, thickness-controlled deposition of the gel and the gel mechanical stability is insured by the EPON SU8 ring (Belmont-Hebert et al., 1998). Before each new cycle of measurements, Hg hemispheres (radius ranging from 5.5 to 6 μm) used as sensing element in this application were electroplated through the gel by applying a −400 mV

deposition potential for 480 s in a 5 mM mercury acetate solution containing 10^{-2} M perchloric acid. After each mercury electrodeposition, the hemispheres were stabilized in 0.1 M $NaNO_3$ using Square Wave Anodic Stripping Voltammetry (SWASV) with the following conditions: precleaning potential of −0.1 V for 1 min; preconcentration potential of −0.9 and −1.1 V for 2 and 5 min, two replicates for each condition; equilibration time of 30 s at −1.1 V. The stripping scan was made from −0.9 or −1.1 V to −0.1 V with a pulse amplitude of 25 mV, a step amplitude of 8 mV, and a frequency of 200 Hz. If required, mercury hemispheres were renewed after Hg reoxidation in 1 M KSCN by linearly scanning the potential from −300 to +300 mV at a scan rate of 5 mV s^{-1}.

2.3. Ad-SWCSV measurements of the dynamic Co-nioxime fraction

The Ad-SWCSV measurements were performed using a Voltametric *In situ* Profiling system (VIP; Tercier et al., 1998) controlled by a laptop computer. An external in-house acid-washed Plexiglas standard cell, incorporating a Hg-GIME as well as Metrohm Ag/AgCl/3 M KCl//0.1 M NaCl suprapur reference and a Platinum (Pt) counter electrodes, was first used. For final optimization and field evaluation/application, the Hg-GIME was incorporated in the VIP mini flow-through Plexiglas cell (www.Idronaut.it). The reference and counter electrodes, respectively, consisted of mini-sized in-house Ag/AgCl/sur-saturated KCl gel reference and a platinum rod electrodes (Idronaut S.r.l). An external double-head peristaltic pump enables on-line mixing of the buffered ligand solution (0.2 M borate pH 8.5, 5.10^{-5} M Nioxime), contained in a surgical bag, with the natural sample (¼ buffered solution, ¾ natural sample). The parameters used in Ad-DPCSV on standard mercury hanging drop macroelectrodes (Metrohm) were optimized for Ad-SWCSV on Hg-GIME. The optimized parameters together with the measurement steps performed are given in Table 1. After each measurement a background scan was recorded, using the same parameters, but with shortened preconcentration time (10 s). The background scan was subtracted from the stripping scan to obtain a corrected final analytical scan with improved signal resolution. Since some trace metals (*i.e.*, Cu, Cd, Pb and Zn) capable of forming an amalgam with mercury can be preconcentrated at the Hg-GIME during the cleaning step, a SWASV is performed after each Ad-SWCSV measurement to reoxidize these metals and clean the Hg-GIME. Experiments were performed with and without oxygen elimination. Oxygen elimination was achieved by bubbling dinitrogen (N_2) in the samples.

2.4. Field test area and sample collection

Field application and evaluation were performed on 20 May 2022 in La Leyre River–Arcachon Bay continuum (France). The Arcachon Bay, located ~100 km to the south of the Gironde Estuary mouth, is a mesotidal lagoon (Fig. 1). This lagoon represents an important breeding ecosystem for regional seafood production, especially oysters. La Leyre River (116 km length, 1700 km^2 basin size) is the main freshwater affluent of the Arcachon Bay contributing 80 % of the annual freshwater input volume (average 1.25×10^6 m^3) to the bay. Samples were collected from La Leyre river (stations A to D) and Arcachon Bay (stations E to H; Fig. 1) and stored in acid-precleaned polyethylene bottles (1 L). Sampling was performed using in-house 12 V peristaltic pump and acid-precleaned Teflon tubing. Aliquots of the raw collected samples were used for on-board preparation of three different fractions: raw sample (no filtration) and samples filtered on 0.2 µm and 0.02 µm pore size membranes (cellulose nitrate, Sartorius; alumina-based membrane, Whatman). The three collected fractions were stored in pre-cleamed 50 mL polyethylene bottles, immediately acidified (0.02 % HNO_3 suprapur, Merck) and stored in a cold box. At the on-site laboratory, the samples were stored at 4 °C prior ICP-MS analysis. A last aliquot of the raw samples was used on site for the quantification of the mobile and labile (dynamic) Co-nioxime fraction using the Hg-GIME VIP. The Hg-GIME VIP was calibrate in the field laboratory the day before deployment.

Table 1
Summary of the Ad-SWCSV protocol for the determination of the dynamic Co-nioxime fraction.

External cell Co Ad-SWCSV protocol	Flow-through cell Co Ad-SWCSV protocol
Gel equilibration: 300 s	Pump on: 180 s
SW stripping and background parameters:	Gel equilibration: 300 s
– E initial: −700 mV	Pump on: 30 s
– E final: −1300 mV	SW stripping and background parameters:
– Pulse amplitude: 25 mV	– E initial: −700 mV
– Step amplitude: 4 mV	– E final: −1300 mV
– Frequency: 200 Hz	– Pulse amplitude: 25 mV
Cell: On	– Step amplitude: 4 mV
Cleaning: E = −1200 mV; t = 30 s	– Frequency: 200 Hz
Preconc.: E = −700 mV; t = 90 s	Cell: On
Equilibration: E = −700 mV; t = 10 s	Cleaning: E = −1200 mV; t = 30 s
Stripping measurement	Preconc.: E = −700 mV; t = 90 s
Cleaning: E = −1200 mV; t = 30 s	Equilibration: E = −700 mV; t = 10 s
Equilibration: E = −700 mV; t = 10 s	Stripping measurement
Background measurement	Cleaning: E = −1150 mV; t = 30 s
Cell: Off	Equilibration: E = −700 mV; t = 10 s
Data storage (internal memory) and transfer (computer)	Background measurement
SW stripping and background parameters:	Cell: Off
– E initial: −1200 mV	Data storage (internal memory) and transfer (computer)
– E final: −200 mV	SW stripping and background parameters:
– Pulse amplitude: 25 mV	– E initial: −1200 mV
– Step amplitude: 8 mV	– E final: −200 mV
– Frequency: 200 Hz	– Pulse amplitude: 25 mV
Cell: On	– Step amplitude: 8 mV
Cleaning: E = −100 mV; t = 60 s	– Frequency: 200 Hz
Preconc.: E = −1200 mV; t = 120 s	Cell: On
Equilibration: E = −1200 mV; t = 60 s	Cleaning: E = −100 mV; t = 60 s
Stripping measurement	Preconc.: E = −1200 mV; t = 120 s
Cleaning: E = −100 mV; t = 60 s	Equilibration: E = −1200 mV; t = 60 s
Equilibration: E = −1200 mV; t = 60 s	Stripping measurement
Background measurement	Cleaning: E = −100 mV; t = 60 s
Cell: Off	Equilibration: E = −1200 mV; t = 60 s
Data storage (internal memory) and transfer (computer)	Background measurement
	Cell: Off
	Data storage (internal memory) and transfer (computer)

ICP-MS measurements of the various collected samples enabled to determine the operationally defined total (Co_{Tot}) (raw samples) and total dissolved <0.2 µm ($Co_{0.2}$) and <0.02 µm ($Co_{0.02}$) fractions. The voltammetric and ICP-MS data were coupled to define four specific homologous metal fractions, as follows: (1) The Co_{Dyn} obtained by direct Hg-GIME Ad-SWCSV measurements and representing the fraction of Co available for bio-uptake; (2) The small colloidal Co species (Co_{SCol}) obtained by subtracting Co_{Dyn} from $Co_{0.02}$ and including the metals adsorbed on small inorganic colloids or forming inert complexes with organic ligands; (3) The inorganic and organic coarse-colloidal Co species (Co_{CCol}) obtained by subtracting $Co_{0.02}$ from $Co_{0.2}$; and (4) The acid-extractable particulate Co (Co_{Par}) obtained by subtraction of $Co_{0.2}$ from Co_{Tot}.

To evaluate and validate our Ad-SWCSV procedure, back to the laboratory, two 0.2 µm samples were collected at stations A and E in pre-cleaned polyethylene bottles. One aliquot was stored at natural pH and the second at pH 1. One aliquot of the pH 1 samples were UV-irradiated at 90 °C during 4 h to decompose the organic matter and assess the total dissolved Co(II) concentration recorded by Ad-SWCSV after reajustment of the pH at appropriate values (see Section 3.4). A second aliquot of the pH 1 samples was analyzed by ICP-MS. The total dissolved Co(II) concentrations (Co_{Tot}) determined by voltammetry and ICP-MS were then compared. The non-acidified and non-UV-irradiated samples (stations A–H) were analyzed to assess the dynamic Co-nioxime concentration at each station and evaluate the proportion of such fraction in comparison

Fig. 1. Map of the La Leyre River and Arcachon Bay location and of the sampling sites associated with a table of their coordinates.

with the total dissolved one.

3. Results and discussion

3.1. Influence of nioxime concentration and pH on the Hg-GIME Ad-SWCSV signal

The influence of the nioxime concentration on Co(II) sensitivity was determined in synthetic media (0.02 M $NaNO_3$ and 0.04 M borate). In the literature, the typically used nioxime (or DMG) concentration is equal or higher than 10^{-5} M (Adeloju and Hadjichari, 1999; Alves et al., 2013). The use of high concentrations of nioxime was never an issue in these previous work since the authors wanted to determine the total dissolved Co(II) concentration in UV-irradiated samples. Our objective here is the direct quantification of the nioxime-labile Co(II) concentration in the natural environments. Since the use of a ligand can modify the Co speciation by competition with natural ligands, the concentration of nioxime in solution should be as low as possible to minimize this competition effect but sufficient to reach appropriate sensitivity. Nioxime concentrations ranging from 10^{-8} up to 5.10^{-5} M was therefore selected and evaluated at two different pH values: pH 8.5 close to the natural pH of fresh and marine waters (see below for more details) and pH 9.2 typically used in previous work for Co(II) detection by AdCSV using nioxime or DMG.

At both pH values, the Co(II) peak intensity increased with the increasing nioxime concentrations from 10^{-8} up to 10^{-6} M (Fig. 2). At pH 8.5, the Co(II) peak intensity levelled off and remained constant for nioxime concentrations between 10^{-5} and 5.10^{-5} M (Fig. 2), while at pH 9.2 a significant current drop was observed. These results suggest that the usual pH 9.2 used in previous studies does not give optimal sensitivity.

Based on the results obtained at pH 8.5, a nioxime concentration of 10^{-5} M was selected for all further experiments. For measurements using the flow-through cell, the VIP multi-channel peristaltic pump enables controlled online mixing of the nioxime solution with the natural samples at a 1:4 ratio. A 4.10^{-5} M nioxime solution was therefore stored in the surgical bag.

The influence of pH on the Hg-GIME Ad-SWCSV Co(II) signal and sensitivity was further studied in synthetic media (0.02 M $NaNO_3$ and 0.04 M borate) and UV-irradiated seawater samples. The pH values ranged from typically 7.46 up to 9.25. In synthetic media, the peak potential for reduction of Co(II) adsorbed shifted to more negative potential with increasing pH (from −1000 to −1112 mV, Fig. 3A). The predicted logarithmic acid dissociation constant (pKa) of nioxime is around 10.70 ± 0.20 while the logarithmic complex formation constant ($\log\beta_2$) of the 1:2 Co-nioxime complex is estimated to be in the range of 16 (Zhang et al., 1990) to 18.1 (Ellwood and van den Berg, 2001). Based on this, the observed shift in the peak potential suggests that an increased amount of Co-nioxime complexes are formed with increasing pH owing to reduced hydrogen ion competition with Co(II) for complexation with nioxime. In contrast, in seawater, the peak potential of Co(II) was at −1150 mV (Fig. 3B) and independent of pH. These results suggest that, in seawater, the 1:2 Co-nioxime complexe is the main complex formed independently of the pH. The absence of hydrogen ion competition might possibly be explained by a stabilization of the Co-nioxime complex by chloride. This hypothesis is however still to be verified, but this was out of the scope of this paper.

In synthetic media, the peak current intensity increased with pH up to pH 8.99 and decreased for a 9.25 pH solution (Figs. 3A, 4A left).

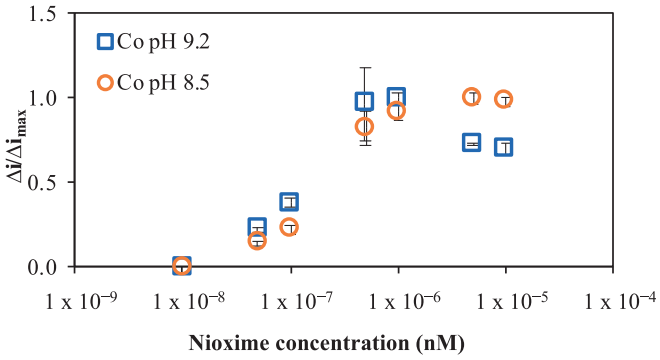

Fig. 2. Influence of nioxime concentration on the Co peak intensity in a solution containing 8 nM Co at both pH 8.5 (orange open circle) and 9.2 (blue open square). Peak intensities were normalized by the highest peak intensity. (For interpretation of the references to colour in this figure legend, the reader is referred to the web version of this article.)

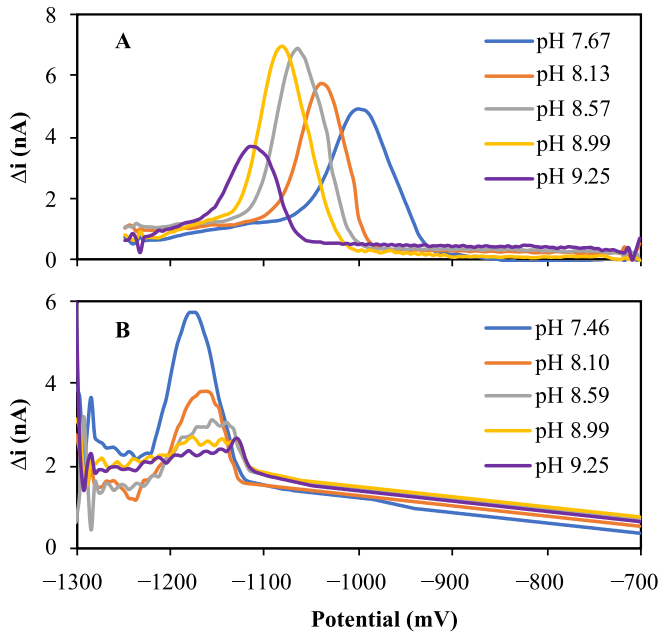

Fig. 3. Co(II) sensitivity in synthetic media (A) and UV-irradiated seawater (B) as a function of pH. The nioxime concentration was 10^{-5} M in both media while the Co(II) concentration was 8 nM in the synthetic media and 2 nM in seawater.

Visual MINTEQ (vers. 3.1) speciation modeling software, predicts that the sum of the inorganic Co species expected to be dynamic (*i.e.* free metal ions, nitrate complexes; Buffle and Tercier-Waeber, 2005) represents >95 % of the total Co(II) for pH up to 8.6. It then decreased owing to the formation of inert complexes in a proportion ≥ 20 % for pH ≥ 9 (Fig. 4A right). This suggests that the variation in the observed Co(II) peak current intensities (Fig. 4A left) is mainly controlled by the decrease in hydrogen ion competition up to pH 9 and by the formation of Co-hydroxide complexes above pH 9.2. In UV-irradiated seawater, the Co(II) peak intensity decreased with increasing pH for the entire range of pH (Figs. 3B, 4B). Formation of inert hydroxide complexes alone cannot explain this decrease as shown by the speciation predicted by Visual MINTEQ based on major truly dissolved ions (Fig. 4B right). UV-irradiation efficiently mineralizes organic compounds but does not influence the concentration of small colloids. Metal desorption/adsorption processes on these small colloids are strongly influenced by pH in the range tested (*e.g.* Tercier-Waeber et al., 2009, 2012) and thus might explain the trends observed.

Overall, these results confirmed that the usual pH used in the literature (pH 9.2) is not the most suitable. They also demonstrated that the speciation of both nioxime and Co must be considered to optimize the parameters to calibrate the Co(II) reduction signals recorded on Hg-GIME by Ad-SWCSV, see below.

3.2. Sensor sensitivity and limit of detection

Calibrations in synthetic and UV-irradiated fresh and marine samples were performed to determine sensitivity and detection limits obtained in various media. The experiments performed at different pH demonstrated that for calibration in synthetic media a pH of 8.5 is optimal to reach good sensitivity and minimize the formation of inert Co-hydroxide complexes. For calibration in UV-irradiated natural samples, pH and added Co(II) concentrations used should be close to their values in natural samples. Since the pH values of freshwater ranged from 7 to 9.5 and of marine waters from 8 to 8.3, pH values of 8.5 and 8.1 were used for calibration in UV-irradiated fresh and marine samples, respectively. The added Co(II) concentrations ranged from 1 to 12 nM in synthetic media (Fig. 5A) and, respectively, from 1 to 8 nM (Fig. 5B) and 1 to 4 nM (Fig. 5C), in UV-irradiated fresh and marine samples. Examples of calibration curves obtained under the selected conditions are given in Fig. 5.

The observed sensitivities and limits of detection (LOD) are summarized in Table 2. In synthetic solution at pH 8.5 a sensitivity of 0.47 ± 0.01 nA nM^{-1} min^{-1} was obtained. Slightly lower sensitivities were observed for calibrations in UV-irradiated fresh and marine waters at pH 8.5 and 8.1 (0.34 ± 0.01 nA nM^{-1} min^{-1} and 0.35 ± 0.02 nA nM^{-1} min^{-1}, respectively). The limit of detections, calculated as 3× the standard deviation of the intercept over the slope of the calibration curve, were below the nM level and comparable within analytical errors for the three media (Table 1). To increase the sensitivity and decrease the limit of detection, the preconcentration time can be increased as demonstrated with the example in freshwater (Table 2). The limit of detection obtained with a preconcentration time of 420 s was 88 ± 8 pM.

As mentioned above, total dissolved Co(II) concentrations in freshwater can be as low as 0.1 nM and reach up to 1.28 mM (Kosiorek, 2019). In sea water, Co(II) concentrations range from 0.017 nM in the open sea to 12.8 nM in coastal areas (Kosiorek, 2019; Morley et al., 1997). The developed analytical method is therefore promising to monitor Co(II) concentration available for bio-uptake in surface and costal area and detect an anomaly due to anthropogenic releases.

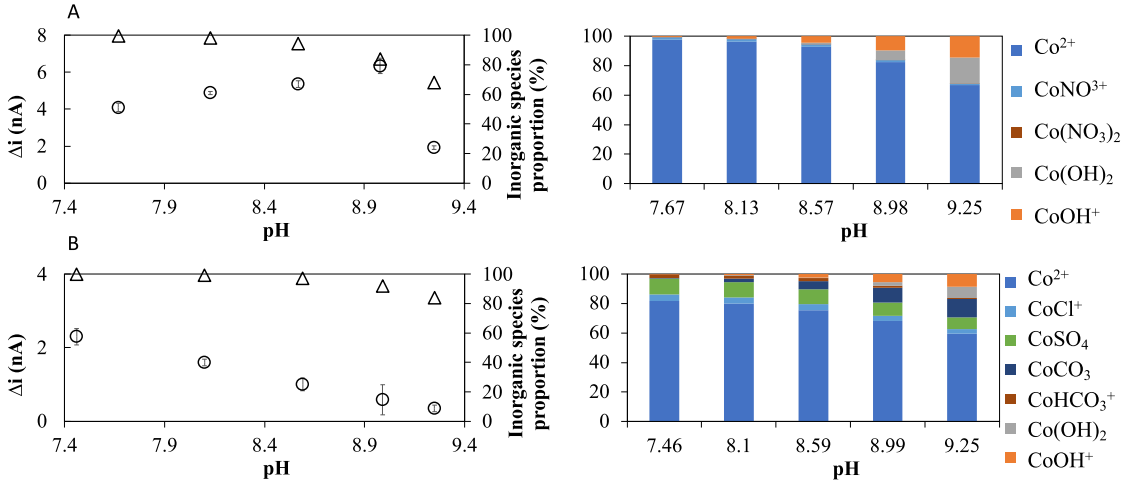

Fig. 4. Intensity of the Co(II) peak recorded by Ad-SWCSV (open circle) as well as the simulated sum of inorganic Co species percentage (open triangle) in the range of the studied pH, in the synthetic media (A) and seawater (B).

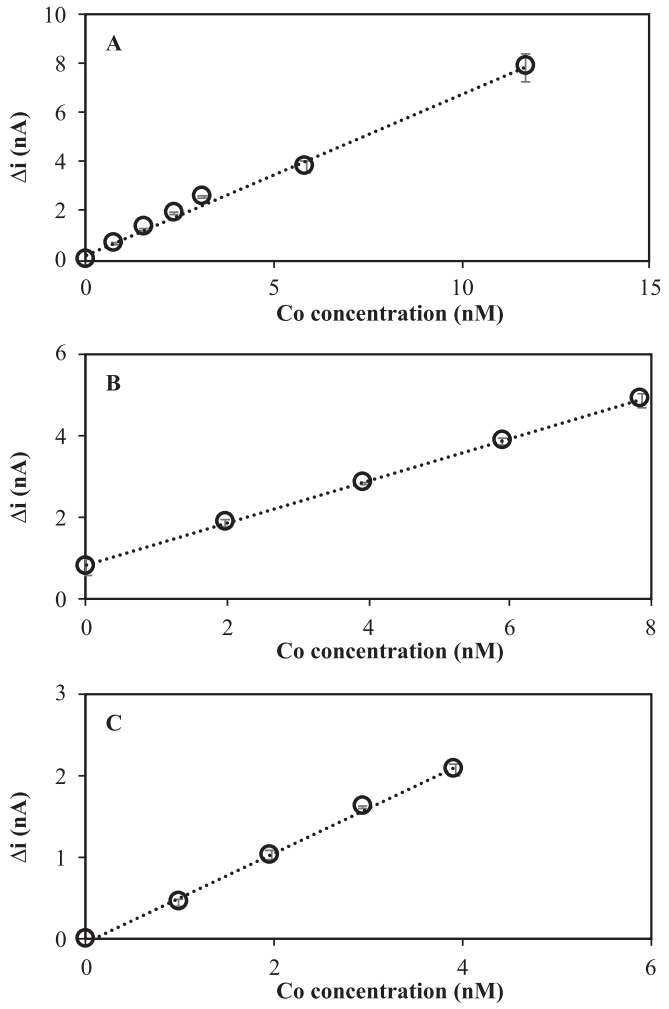

Fig. 5. Co(II) calibration in (A) the synthetic media at pH 8.5 (0.02 M $NaNO_3$ and 0.04 M Borate), and UV-irradiated (B) freshwater buffered at pH 8.5 (0.02 M $NaNO_3$ and 0.04 M Borate) and (C) in seawater at natural pH 8.1.

Table 2
Sensitivity for Co(II) in the synthetic media, and UV-irradiated fresh and marine waters associated with the calculated limit of detection in nM.

Media	pH	Sensitivity (nA nM^{-1} min^{-1})	LOD 90s (nM)	LOD 420 s (nM)
Synthetic (n = 3)	8.5	0.47 ± 0.01	0.30 ± 0.03	–
Freshwater (n = 2)	8.5	0.34 ± 0.01	0.29 ± 0.01	0.088 ± 0.008
Seawater (n = 3)	8.1	0.35 ± 0.02	0.27 ± 0.06	–

3.3. Influence of temperature

Temperature influences the diffusion coefficient (D) and therefore the mass transport of species toward sensor surface (Bard and Faulkner, 2001). Since the temperature of aquatic systems may vary between usually 25 to 4 °C as a function of the depth and seasons, it is necessary to determine an experimental temperature correction factor to apply to correct the voltammetric signals recorded *in situ*. It has already been demonstrated in previous papers (Belmont-Hebert et al., 1998; Touilloux et al., 2015) that Eq. (1), derived from the Arrhenius' law and the direct proportionality between current intensity and D at microsized electrodes, can be used to achieve this.

$$i \propto D \rightarrow i = i_0 e^{-\frac{\Delta G}{RT}} \quad (1)$$

where ΔG correspond to the free enthalpy, T the temperature and R the universal gas constant.

Eq. (1) suggests a linear relationship between ln (i) and 1/T, and that ΔG/R, which is the temperature effect correction factor, can be experimentally determined from the slope of the linear curve obtained. This experimental temperature effect correction factor can later be applied to correct the influence of temperature on the currents recorded *in situ* by voltammetry on microelectrodes using Eq. (2).

$$i_{T_{room}} = i_{T_{in\ situ}} e^{\frac{\Delta G}{R}\left(\frac{1}{T_{room}} - \frac{1}{T_{in\ situ}}\right)} \quad (2)$$

where $T_{in\ situ}$ is the temperature of the sample measured *in situ*, T_{room} is the temperature used for calibration, $i_{Tin\ situ}$ is the current measured *in situ* with $T_{in\ situ}$ and i_{Troom} is the corrected current for T_{room}.

The experiments were performed with a solution containing 12 nM Co(II) and 10^{-5} M nioxime. The experiments were performed in triplicates using a linear ramp from 25 °C to 5 °C and 5 °C to 25 °C with a step of 5 °C.

As expected, a linear relationship was observed between ln(i) and 1/T in the three studied media (Fig. 6). The correction temperature effect factors, ΔG/R, determined from the slopes was found to be (−4465 ± 188), (−4485 ± 234) and (−4044 ± 301) in the synthetic media, freshwater, and seawater, respectively. These values are higher that the theoretical value E_a/R (with E_a being the activation energy) of −2555 given by the Stokes–Einstein equation (Belmont-Hebert et al., 1998) where the linear relationship is determined between ln(D) and 1/T. It may be concluded that the peak current behaves as for a not entirely reversible system under the fast SWAdCSV scan rate conditions used (0.8 V s^{-1}).

3.4. Analytical method evaluation and validation

The evaluation and validation of analytical methods prior their field application are a pre-requisite to insure the reliability of field monitoring data. Toward this aim, Co(II) quantification by Ad-SWCSV in presence of nioxime were applied to samples collected at station A (freshwater) and E (seawater) prior (Co_{Dyn}) and after ($Co_{0.2}$) UV-irradiation. For UV-irradiation, samples were acidified at pH 1. At the end of the irradiation, the pH was adjusted at 8.5 for sample A and 8.1 for sample E. The Hg-GIME Ad-SWCSV measurements were performed after samples re-equilibration over-night. In parallel an aliquot of samples collected at stations A and E was acidified and analyzed by ICP-MS

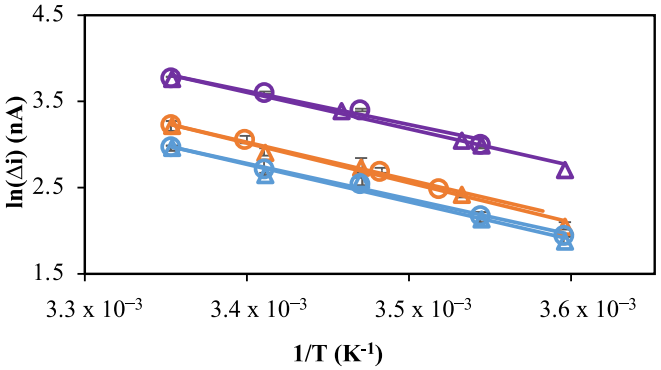

Fig. 6. Influence of the temperature on the Co(II) stripping peak current intensities in synthetic media (violet), freshwater (orange) and seawater (blue). Each experiment has been done from 25 °C down to 5 °C (open circles) and form 5 °C up to 25 °C (open triangles) in triplicates. (For interpretation of the references to color in this figure legend, the reader is referred to the web version of this article.)

($Co_{0.2}$). Results obtained by ICP-MS and Ad-SWCSV after UV-irradiation were then compared.

$Co_{0.2}$ measured by ICP-MS in both samples were comparable, within analytical error the one measured by Ad-SWCSV on Hg-GIME after UV-irradiation (Table 3). This validates our analytical methodology. Co_{Dyn} determined in the raw samples by Ad-SWCSV on Hg-GIME were lower than $Co_{0.2}$ measured after UV-irradiation, (Table 3). Co_{Dyn} represented only 24 and 26 % of $Co_{0.2}$ measured by ICP-MS. These results confirm that our sensor only detects a small fraction of the total dissolved Co(II) concentration. They also suggest a low competition of nioxime with non-dynamic natural organic and inorganic cobalt sorbents.

3.5. Field application in the Leyre River–Arcachon Bay continuum

Due to time constraints, Hg-GIME VIP measurements in the Arcachon Bay were performed on-board in freshly collected samples and at natural pH that ranged from 8 to 8.1. Samples collected in La Leyre River were analyzed in the field laboratory within a maximum of 12 h after sampling upon buffering the sample pH to 8.5. The concentrations of the different fractions of Co(II) measured along the transect from La Leyre river (stations A to D) and the Arcachon Bay toward the open ocean (stations E to H) at ebb tide and the resulting Co(II) speciation are reported in Fig. 7A and B, respectively.

Co_{Tot} were similar at stations A and B (around 4 nM), increased at stations C and D (up to 8.7 nM) and then decreased down to 3.05 nM toward open sea reflecting a dilution effect (Fig. 7A). The increase of Co_{Tot} observed at stations C and D was correlated with an increase of ammonium concentration (Fig. 7A and C). Ammonium is a compound of fertilizer used in soils. This suggests that the observed Co_{Tot} and NH_4^+ might result from their runoff from the surrounding land following an intense rainy episode occurring the day before. $Co_{0.2}$ was decreasing from station A (4.48 nM) to H (1.21 nM) reflecting a dilution effect along the transect of freshwater Co(II) sources (Fig. 7A). The same trends was observed for $Co_{0.02}$ with concentrations ranging from 4.36 nM at station A to 1.29 nM at station H. Co_{Dyn} increased from station A (1.08 ± 0.13 nM) to B (1.82 ± 0.06 nM) and was lower than the limit of detection at stations C and D which might be explained by Co(II) adsorption on suspended particles issued from the surrounding land run-off. This hypothesis is supported by the increase of Co_{Par} observed at these stations (Fig. 7B). Finally, in the bay (stations E to H) Co_{Dyn} was overall similar (0.7 ± 0.2 nM) (Fig. 7A). Focusing on the proportions of the different fractions, one can see that Co_{Par} did not play a significant role in the Co speciation at station A (0 %) and B (3 %) but did at station C and D (50 and 56 % respectively) (Fig. 7B). On the contrary, in the bay, the particulate fraction Co_{Par} represented 25 % at stations F, G and H and up to 39 % at station E of the total Co(II) concentration (Fig. 7B). These results suggest aggregation of the Co colloids due to increase in chloride concentration (Tercier-Waeber et al., 2012).

Co_{CCol} did not represented a significant fraction of the total Co(II) concentration along the whole transect (<14 %) (Fig. 7B). This indicates that coarse colloids did not play a significant role in the Co(II) speciation. In contrast, Co_{SCol} represented from 26 % (station G) up to 72 % (station A) of the total Co concentration (Fig. 7B). This finding highlights that nano-sized colloids play a major role in Co(II) transport. Finally, the contribution of Co_{Dyn} to Co_{Tot} varied significantly at each station. It represented from ~0 up to 48 % in La Leyre River and from 17 % up to 47 % in the Bay (Fig. 7B). These results demonstrate that it is important to measure in real time this fraction which can evolve in space depending on the composition of the medium. In addition, regarding the Australian and New Zealand directives, Co_{Dyn} measured at all marine stations (stations E to H) were higher than the defined threshold for 99 % species protection (*i.e.* 0.085 nM). This demonstrated the need of metal-hazardous bioavailable-assessment sensing tool for efficient survey and protection of important socio-economic coastal areas such as the Arcachon Bay.

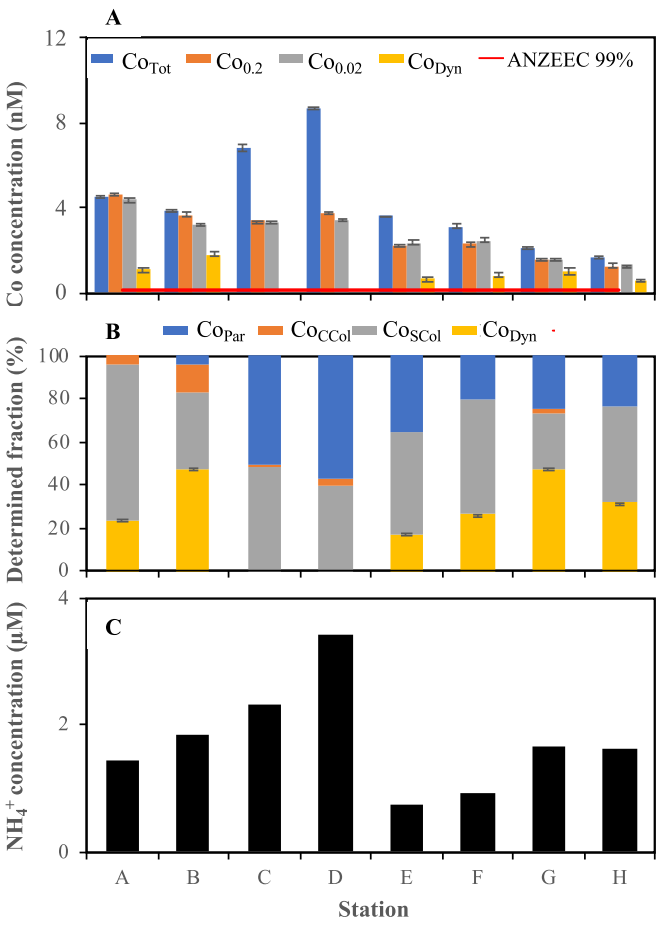

Fig. 7. (A) Spatial variation of Co_{Tot}, $Co_{0.2}$, $Co_{0.02}$ and Co_{dyn} associated with the maximum Co(II) concentration that should not be exceed to protect 99 % of the marine species. (B) proportion of the different Co fractions: Co_{Par} associated to suspended particles, Co_{CCol} associated to coarse colloids (between 0.02 and 0.2 µm), Co_{SCol} associated to small colloids (between 4 nm and 0.02 µm) and Co_{Dyn} available for bio-uptake. (C) Ammonium concentrations (measured by spectrophotometry, Perkin Elmer) along the transect profile performed from stations A to H.

Table 3
Total dissolved Co(II) concentration in freshwater and seawater samples measured by ICP-MS and by Hg-GIME Ad-SWCSV after UV-irradiation, as well as the dynamic Co-nioxime concentration in raw samples.

	ICP-MS $Co_{0.2}$ (nM)	Hg-GIME Ad-SWCSV		$Co_{0.2}$ recovery Ad-SWCSV/ICP-MS (%)	Co_{Dyn}/ $Co_{0.2}$ ICP-MS (%)
		$Co_{0.2}$ (nM)	Co_{Dyn} (nM)		
Freshwater	4.58 ± 0.05	5.60 ± 0.47	1.08 ± 0.13	122 ± 9	24
Seawater	2.34 ± 0.06	2.48 ± 0.18	0.61 ± 0.09	106 ± 5	26

4. Conclusion

For the first time ever, we successfully quantify *on-field* the potentially bioavailable Co(II) concentration in natural waters. For this purpose, we successfully developed an analytical approach based on the dynamic Co(II) detection on Hg-GIME by using Ad-SWCSV in the presence of nioxime. The parameters influencing the voltammetric signal were investigated. The optimal nioxime concentration and pH value were determined for both fresh and seawater. A temperature correction

factor was determined. The results obtained in UV-irradiated natural samples with the developed technique were compared with traditional ICP-MS measurements which allowed to validate our methodology. The optimized analytical methodology was successfully applied in the Arcachon Bay and its main effluent, La Leyre River, using Hg-GIME incorporated in the VIP submersible probe. The results have demonstrated that Co(II) concentration and its spatial variation can be monitored at sub-nanomolar level. They also demonstrated that La Leyre River is a source of several Co(II) species in the Arcachon Bay. Moreover, the determined dynamic Co(II) concentrations along the continuum were hazardous for aquatic biota. Finally, the developed method is generic and thus offer opportunity to detect a wider range of trace metals in the near future. Especially, we investigated if the methodology reported here is also suitable for the quantification of the potentially bioavailable fraction of Ni(II). The results are reported elsewhere (Creffield et al., 2023).

CRediT authorship contribution statement

Nicolas Layglon: Conceptualization, Methodology, Validation, Formal analysis, Investigation, Writing – original draft, Writing – review & editing, Supervision, Funding acquisition. **Sébastien Creffield:** Validation, Formal analysis, Investigation, Data curation. **Eric Bakker:** Writing – review & editing, Funding acquisition. **Mary-Lou Tercier-Waeber:** Writing – review & editing, Supervision, Project administration, Funding acquisition.

Declaration of competing interest

The authors declare that they have no known competing financial interests or personal relationships that could have appeared to influence the work reported in this paper.

Data availability

Data will be made available on request.

Acknowledgments

This work was financially supported by the Swiss National Science Foundation (Project Number 207373). The authors thank the analytical platform “Majeurs et Métaux traceS” (M&Ms; UMR 5805 EPOC, University of Bordeaux; especially Cécile Bossy) for performing the ICP-MS quantification of dissolved cobalt concentrations and gratefully acknowledge the help of the R/V Planula IV Crew (TGIR FOF).

References

Abdou, M., Tercier-Waeber, M.-L., 2022. New insights into trace metal speciation and interaction with phytoplankton in estuarine coastal waters. Mar. Pollut. Bull. 181, 113845 https://doi.org/10.1016/j.marpolbul.2022.113845.

Abdou, M., Tercier-Waeber, M.-L., Dutruch, L., Bossy, C., Pougnet, F., Coynel, A., Bakker, E., Blanc, G., Schäfer, J., 2022. Estuarine dissolved speciation and partitioning of trace metals: a novel approach to study biogeochemical processes. Environ. Res. 208, 112596 https://doi.org/10.1016/j.envres.2021.112596.

Adeloju, S.B., Hadjichari, A., 1999. Simultaneous determination of nickel and cobalt in natural water and sediment samples on an in-situ plated mercury film electrode by adsorptive cathodic stripping voltammetry. Anal. Sci. 15, 95–100. https://doi.org/10.2116/analsci.15.95.

Alves, G.M.S., Magalhães, J.M.C.S., Soares, H.M.V.M., 2013. Simultaneous determination of nickel and cobalt using a solid bismuth vibrating electrode by adsorptive cathodic stripping voltammetry. Electroanalysis 25, 1247–1255. https://doi.org/10.1002/elan.201200643.

Anderson, R., Mawji, E., Cutter, G., Measures, C., Jeandel, C., 2014. GEOTRACES: changing the way we explore ocean chemistry. Oceanography 27, 50–61. https://doi.org/10.5670/oceanog.2014.07.

ANZEEC, 2000. Australian and New Zealand Guidelines for fresh and marine water quality. In: Natl. Water Qual. Manag. Strategy.

Bard, A.J., Faulkner, L.R., 2001. Electrochemical Methods: Fundamentals And Applications, second ed. John Wiley, New York, USA.

Belmont-Hebert, C., Tercier, M.L., Buffle, J., Fiaccabrino, G.C., Rooij, N.F., Koudelka-Hep, M., 1998. Gel-integrated microelectrode arrays for direct voltammetric measurements of heavy metals in natural waters and other complex media. Anal. Chem. 70, 2949–2956. https://doi.org/10.1021/ac971194c.

Buffle, J., Tercier-Waeber, M.-L., 2005. Voltammetric environmental trace-metal analysis and speciation: from laboratory to in situ measurements. TrAC Trends Anal. Chem. 24, 172–191. https://doi.org/10.1016/j.trac.2004.11.013.

Buffle, J., Tercier-Waeber, M.-L., 2000. In situ voltammetry: concepts and practice for trace analysis and speciation, chap. 9. In: Situ Monitoring of Aquatic Systems. Chemical Analysis And Speciation. Wiley, Chichester.

Bundy, R.M., Tagliabue, A., Hawco, N.J., Morton, P.L., Twining, B.S., Hatta, M., Noble, A.E., Cape, M.R., John, S.G., Cullen, J.T., Saito, M.A., 2020. Elevated sources of cobalt in the Arctic Ocean. Biogeosciences 17, 4745–4767. https://doi.org/10.5194/bg-17-4745-2020.

Cindric, A.-M., Cukrov, N., Durrieu, G., Garnier, C., PiZeta, I., Omanovic, D., 2017. Evaluation of discrete and passive sampling (diffusive gradients in thin-films–DGT) approach for the assessment of trace metal dynamics in marine waters–a case study in a small harbor. Croat. Chem. Acta 90. https://doi.org/10.5562/cca3163.

Collins, R.N., Kinsela, A.S., 2010. The aqueous phase speciation and chemistry of cobalt in terrestrial environments. Chemosphere 79, 763–771. https://doi.org/10.1016/j.chemosphere.2010.03.003.

Creffield, S., Tercier-Waeber, M.-L., Gressard, T., Bakker, E., Layglon, N., 2023. On-chip antifouling gel-integrated microelectrode arrays for in situ high-resolution quantification of the nickel fraction available for bio-uptake in natural waters. Molecules 28, 1346. https://doi.org/10.3390/molecules28031346.

Ellwood, M.J., van den Berg, C.M.G., 2001. Determination of organic complexation of cobalt in seawater by cathodic stripping voltammetry. Mar. Chem. 75, 33–47. https://doi.org/10.1016/S0304-4203(01)00024-X.

Gibbon-Walsh, K., Salaün, P., van den Berg, C.M.G., 2010. Arsenic speciation in natural waters by cathodic stripping voltammetry. Anal. Chim. Acta 662, 1–8. https://doi.org/10.1016/j.aca.2009.12.038.

Holmes, J., Pathirathna, P., Hashemi, P., 2019. Novel frontiers in voltammetric trace metal analysis: towards real time, on-site, in situ measurements. TrAC Trends Anal. Chem. 111, 206–219. https://doi.org/10.1016/j.trac.2018.11.003.

Illuminati, S., Annibaldi, A., Truzzi, C., Tercier-Waeber, M.L., Noel, S., Braungardt, C.B., Achterberg, E.P., Howell, K.A., Turner, D., Marini, M., Romagnoli, T., Totti, C., Confalonieri, F., Graziottin, F., Buffle, J., Scarponi, G., 2019. In-situ trace metal (Cd, Pb, Cu) speciation along the Po River plume (Northern Adriatic Sea) using submersible systems. Mar. Chem. 212, 47–63. https://doi.org/10.1016/j.marchem.2019.04.001.

Kokkinos, C., Economou, A., 2016. Microfabricated chip integrating a bismuth microelectrode array for the determination of trace cobalt(II) by adsorptive cathodic stripping voltammetry. Sens. Actuators B Chem. 229, 362–369. https://doi.org/10.1016/j.snb.2016.01.148.

Kosiorek, M., 2019. Effect of cobalt on the environment and living organisms - a review. Appl. Ecol. Environ. Res. 17 https://doi.org/10.15666/aeer/1705_1141911449.

Layglon, N., Abdou, M., Massa, F., Castellano, M., Bakker, E., Povero, P., Tercier-Waeber, M.-L., 2022. Speciation of Cu, Cd, Pb and Zn in a contaminated harbor and comparison to environmental quality standards. J. Environ. Manag. 317, 115375 https://doi.org/10.1016/j.jenvman.2022.115375.

Masson, M., Tercier-Waeber, M.L., 2014. Trace metal speciation at the sediment-water interface of Vidy Bay: influence of contrasting sediment characteristics. Aquat. Sci. 76, 47–58. https://doi.org/10.1007/s00027-013-0323-6.

Morley, N.H., Burton, J.D., Tankere, S.P.C., Martin, J.-M., 1997. Distribution and behaviour of some dissolved trace metals in the western Mediterranean Sea. Deep-Sea Res. II Top. Stud. Oceanogr. 44, 675–691. https://doi.org/10.1016/S0967-0645(96)00098-7.

Niyogi, S., Wood, C.M., 2004. Biotic ligand model, a flexible tool for developing site-specific water quality guidelines for metals. Environ. Sci. Technol. 38, 6177–6192. https://doi.org/10.1021/es0496524.

Pađan, J., Marcinek, S., Cindrić, A.-M., Layglon, N., Garnier, C., Salaün, P., Cobelo-García, A., Omanović, D., 2020. Determination of sub-picomolar levels of platinum in the pristine Krka River estuary (Croatia) using improved voltammetric methodology. Environ. Chem. 17, 77. https://doi.org/10.1071/EN19157.

Pađan, J., Marcinek, S., Cindrić, A.-M., Layglon, N., Lenoble, V., Salaün, P., Garnier, C., Omanović, D., 2019. Improved voltammetric methodology for chromium redox speciation in estuarine waters. Anal. Chim. Acta 1089, 40–47. https://doi.org/10.1016/j.aca.2019.09.014.

Saili, K.S., Cardwell, A.S., Stubblefield, W.A., 2021. Chronic toxicity of cobalt to marine organisms: application of a species sensitivity distribution approach to develop international water quality standards. Environ. Toxicol. Chem. 40, 1405–1418. https://doi.org/10.1002/etc.4993.

Smith, K.S., Balistrieri, L.S., Todd, A.S., 2015. Using biotic ligand models to predict metal toxicity in mineralized systems. Appl. Geochem. 57, 55–72. https://doi.org/10.1016/j.apgeochem.2014.07.005.

Tagliabue, A., Hawco, N.J., Bundy, R.M., Landing, W.M., Milne, A., Morton, P.L., Saito, M.A., 2018. The role of external inputs and internal cycling in shaping the global ocean cobalt distribution: insights from the first cobalt biogeochemical model. Glob. Biogeochem. Cycles 32, 594–616. https://doi.org/10.1002/2017GB005830.

Tercier, M.-L., Buffle, J., 1996. Antifouling membrane-covered voltammetric microsensor for in situ measurements in natural waters. Anal. Chem. 68, 3670–3678. https://doi.org/10.1021/ac960265p.

Tercier, M.-L., Buffle, J., Graziottin, F., 1998. A novel voltammetric in-situ profiling system for continuousreal-time monitoring of trace elements in natural waters. Electroanalysis 10, 355–363. https://doi.org/10.1002/(SICI)1521-4109(199805)10:6<355::AID-ELAN355>3.0.CO;2-F.

Tercier-Waeber, M., Buffle, J., 2013. Sensors and voltammetric probes for in situ monitoring of trace elements in aquatic media. In: Fouletier, J., Fabry, P. (Eds.), Chemical And Biological Microsensors. Wiley, pp. 233–285. https://doi.org/10.1002/9781118603871.ch8.

Tercier-Waeber, M.-L., Abdou, M., Fighera, M., Kowal, J., Bakker, E., van der Wal, P., 2021a. In situ voltammetric sensor of potentially bioavailable inorganic mercury in marine aquatic systems based on gel-integrated nanostructured gold-based microelectrode arrays. ACS Sensors 6, 925–937. https://doi.org/10.1021/acssensors.0c02111.

Tercier-Waeber, M.-L., Confalonieri, F., Abdou, M., Dutruch, L., Bossy, C., Fighera, M., Bakker, E., Graziottin, F., van der Wal, P., Schäfer, J., 2021b. Advanced multichannel submersible probe for autonomous high-resolution in situ monitoring of the cycling of the potentially bioavailable fraction of a range of trace metals. Chemosphere 282, 131014. https://doi.org/10.1016/j.chemosphere.2021.131014.

Tercier-Waeber, M.-L., Confalonieri, F., Koudelka-Hep, M., Dessureault-Rompré, J., Graziottin, F., Buffle, J., 2008. Gel-integrated voltammetric microsensors and submersible probes as reliable tools for environmental trace metal analysis and speciation. Electroanalysis 20, 240–258. https://doi.org/10.1002/elan.200704067.

Tercier-Waeber, M.-L., Fighera, M., Abdou, M., Bakker, E., van der Wal, P., 2021c. Newly designed gel-integrated nanostructured gold-based interconnected microelectrode arrays for continuous in situ arsenite monitoring in aquatic systems. Sensors Actuators B Chem. 328, 128996 https://doi.org/10.1016/j.snb.2020.128996.

Tercier-Waeber, M.-L., Hezard, T., Masson, M., Schäfer, J., 2009. In situ monitoring of the diurnal cycling of dynamic metal species in a stream under contrasting photobenthic biofilm activity and hydrological conditions. Environ. Sci. Technol. 43, 7237–7244. https://doi.org/10.1021/es900247y.

Tercier-Waeber, M.-L., Stoll, S., Slaveykova, V., 2012. Trace metal behavior in surface waters: emphasis on dynamic speciation, sorption processes and bioavailability. Arch. Sci. 65, 119–142.

Tercier-Waeber, M.L., Taillefert, M., 2008. Remote in situ voltammetric techniques to characterize the biogeochemical cycling of trace metals in aquatic systems. J. Environ. Monit. 10, 30–54. https://doi.org/10.1039/B714439N.

Touilloux, R., Tercier-Waeber, M.L., Bakker, E., 2015. Antifouling membrane integrated renewable gold microelectrode for in situ detection of As(III). Anal. Methods 7, 7503–7510. https://doi.org/10.1039/C5AY01941A. Uk.

Väänänen, K., Leppänen, M.T., Chen, X., Akkanen, J., 2018. Metal bioavailability in ecological risk assessment of freshwater ecosystems: from science to environmental management. Ecotoxicol. Environ. Saf. 147, 430–446. https://doi.org/10.1016/j.ecoenv.2017.08.064.

Vega, M., van den Berg, C.M.G., 1997. Determination of cobalt in seawater by catalytic adsorptive cathodic stripping voltammetry. Anal. Chem. 69, 874–881. https://doi.org/10.1021/ac960214s.

Wang, Joseph, Wang, Jianyan, Adeniyi, W.K., Kounaves, S.P., 2000. Adsorptive stripping analysis of trace nickel at iridium-based ultramicroelectrode arrays. Electroanalysis 12, 44–47. https://doi.org/10.1002/(SICI)1521-4109(20000101)12:1<44::AID-ELAN44>3.0.CO;2-4.

WCA Environment, 2016. Bioavailability Implementation Forum SETAC Europe – Nantes. Meeting the Challenges of Implementing Bioavailability-Based EQS for Metals.

WCA Environment, 2015. Technical Guidance to Implement Bioavailability-based Environmental Quality Standards for Metals.

WFD-2013/39/EU, 2013. Directive 2013/39/EU, Directive 2013/39/EU of the European Parliament and of the Council of 12 August 2013 amending Directives 2000/60/EC and 2008/105/EC as regards priority substances in the field of water policy. Off. J. Eur. Union.

Xie, X., Stueben, D., Berner, Z., 2005. The application of microelectrodes for the measurements of trace metals in water. Anal. Lett. 38, 2281–2300. https://doi.org/10.1080/00032710500316050.

Zhang, H., Van Den Berg, C.M.G., Wollast, R., 1990. The determination of interactions of cobalt (II) with organic compounds in seawater using cathodic stripping voltammetry. Mar. Chem. 28, 285–300. https://doi.org/10.1016/0304-4203(90)90049-I.

Zhao, C.-M., Campbell, P.G.C., Wilkinson, K.J., 2016. When are metal complexes bioavailable? Environ. Chem. 13, 425. https://doi.org/10.1071/EN15205.